HHS Public Access

Author manuscript

Microvasc Res. Author manuscript; available in PMC 2016 March 01.

Published in final edited form as:

Microvasc Res. 2015 March ; 98: 126–138. doi:10.1016/j.mvr.2015.01.006.

ID3 Contributes to the Acquisition of Molecular Stem Cell-Like Signature in Microvascular Endothelial Cells: Its implication for understanding microvascular diseases

Jayanta K. Das[a], **Norbert F. Voelkel**[b], and **Quentin Felty**[a,*]

[a]Department of Environmental & Occupational Health Florida International University, Miami, FL, USA

[b]Pulmonary and Critical Care Medicine Division and Victoria Johnson Center for Obstructive Lung Diseases, Virginia Commonwealth University, Richmond, VA, USA

Abstract

While significant progress has been made to advance our knowledge of microvascular lesion formation, yet the investigation of how stem-like cells may contribute to the pathogenesis of microvascular diseases is still in its infancy. We assessed whether the inhibitor of DNA binding and differentiation 3 (ID3) contributes to the acquisition of a molecular stem cell-like signature in microvascular endothelial cells. The effects of stable ID3 overexpression and SU5416 treatment — a chemical inducer of microvascular lesions, had on the stemness signature was determined by flow cytometry, immunoblot, and immunohistochemistry. Continuous ID3 expression produced a molecular stemness signature consisting of $CD133^+$ $VEGFR3^+$ $CD34^+$ cells. Cells exposed to SU5416 showed positive protein expression of ID3, VEGFR3, CD34 and increased expression of pluripotent transcription factors Oct-4 and Sox-2. ID3 overexpressing cells supported the formation of a 3-D microvascular lesion co-cultured with smooth muscle cells. In addition, *in vivo* microvascular lesions from SuHx rodent model showed an increased expression of ID3, VEGFR3, and Pyk2 similar to SU5416 treated human endothelial cells. Further investigations into how normal and stem-like cells utilize ID3 may open up new avenues for a better understanding of the molecular mechanisms which are underlying the pathological development of microvascular diseases.

*Correspondence: Quentin Felty, Department of Environmental & Occupational Health, Florida International University, 11200 SW 8th Street AHC5-351, Miami, FL USA. Tel.: 305-348-7785; Fax.: 305-348-4901; Feltyq@fiu.edu.

Competing financial interests: The authors declare no competing financial interests.

Author contributions

J.K.D.: provision of study materials, manuscript writing, collection/assembly of data; N.F.V.: design of animal study, manuscript writing, provision of study material; Q.F.: conception and design, administrative support, financial support, data analysis/interpretation, manuscript writing, and final approval.

Introduction

Prevention and treatment of vascular complications remain a critical problem in the management of many microvascular diseases. It is becoming increasingly recognized that the pathogenesis of microvascular complications, as well as of several macrovascular diseases, includes disordered proliferation of endothelial cells (ECs). There is a strong correlation between susceptibility to micro— and macro—vascular complications, especially in patients with atherosclerosis contributing to renal disease, diabetic retinopathy, and cardiovascular disease (CVD). Furthermore, proliferative microvascular lesions that result from a focal budding of ECs and resemble a renal glomerulus are reported to be an aggressive angiogenic phenotype associated with a poor prognosis in glioblastoma multiforme, non-small cell lung cancer (NSCLC), and severe idiopathic pulmonary arterial hypertension (IPAH) (Rojiani et al., 1996; Tanaka et al., 2003; Tuder et al., 1994a). The resemblance of EC proliferation of pulmonary plexiform lesions to cancer is supported by the fact that ECs in severe IPAH are monoclonal (Lee et al., 1998). The hyper-proliferative, apoptosis-resistant, and monoclonal phenotype observed in ECs that form plexiform lesions has been put in the context of a quasi malignant process which conceptually can accommodate impairment of stem cell differentiation (Rai et al., 2008). The theory that malignant transformation depends on a small population of stem-like cells for proliferation has received much attention, however, there have been few studies which support a pathogenic role for stem cells in vascular proliferative malformations.

There is some evidence that allude to a potential role of inhibitor of differentiation (Id) protein 3 in malignant stemness as well as angiogenesis. For instance, induction of ID3 and ID3-regulated cytokines has been reported to lead to the acquisition of glioma stem cell (GSC) characteristics and angiogenesis (Jin et al., 2011). Since ID3 has been shown to be involved in VEGF-dependent EC proliferation (Sakurai et al., 2004) and based on the previous hypothesis that VEGF signaling mechanisms are associated with both plexiform and glomeruloid lesions (Tuder et al., 2001); it is biologically plausible that ID3 shares a common role in the development of microvascular lesions found in severe forms of PAH as well as in cancer. The transcription regulator ID3 was shown to be up-regulated in the pulmonary vasculature following prolonged exposure of rats to hypoxia (Lowery et al., 2010) and may affect BMP signaling and the proliferation of human pulmonary artery smooth muscle cells (Yang et al., 2013). A number of recent publications associate endothelial progenitor cells and dysfunctional resident mesenchymal stem cells with vascular remodeling associated with PAH (Diller et al., 2010; Gambaryan et al., 2011; Chow et al., 2013). Although direct evidence for the role of ID3 in microvascular lesion formation is lacking, the function of Id proteins to prevent cell commitment raises the question of whether ID3 may exacerbate the formation of microvascular lesions via its contribution to EC stemness.

Improved cell models are critical for understanding the pathogenesis of these types of vascular complications and for testing potential new prevention and treatment modalities for microvascular disease. Our laboratory has recently observed a significant decrease in apoptosis of human cerebral microvascular ECs that overexpress ID3 when compared to wild-type. We postulated that ID3 overexpression contributes to the acquisition of a

molecular stem cell-like signature in human microvascular ECs and when cultured under specific conditions EC $^{ID3+}$ stem-like cells develop lesions that morphologically resemble microvascular proliferative lesions found in other pathologies including cancers and IPAH. Therefore, we developed a stable endothelial cell clone that overexpressed ID3 and determined whether ID3 contributed to the acquisition of a molecular stem cell-like signature. The formation of microvascular lesions has been extensively studied using the SU5416/chronic hypoxia (SuHx) rodent model of severe PAH. A chemical antagonist of VEGFR1 and 2, SU5416, has been implicated in the growth of pulmonary endothelial lesions by expanding surviving $CD34^+$ stem cell-like cells in vitro. Human $CD133^+$ $CD34^+$ cells that also express VEGFR3 were previously reported to constitute a phenotypically and functionally distinct population of endothelial stem cells. Therefore, we compared the following endothelial types EC ^{wt} and EC $^{ID3+}$ to determine the effect of ID3 overexpression or exposure to SU5416— a chemical inducer of microvascular lesions had on the molecular stem cell-like signature.

Materials and Methods

Chemicals and reagents

The chemical SU5416, an inhibitor of VEGFR tyrosine kinase activity, was purchased from Sigma, St Louis, MO. For immunofluorescent imaging, antibodies labeled with Alexa Fluor® dyes 633, 488, and 546 were purchased from Invitrogen Life Technologies, CA. For culture of ECs B27® serum-free supplement was also purchased from Invitrogen Life Technologies. All other reagents are mentioned in the following sections.

Cell culture

The human cerebral microvascular endothelial cell line HCMEC/D3 was obtained from Dr. B. Weksler, Weill Medical College of Cornell University, NY (Weksler et al., 2005); and will be referred to as endothelial wild-type cells (EC ^{wt}) to make a distinction from our endothelial ID3 overexpressing clone (EC $^{ID3+}$). The HCMEC/D3 cells have been shown to retain their EC characteristics with a stable normal karyotype, proliferate in response to endothelial growth factors, and form capillary tubes in matrix but no colonies in soft agar (Weksler et al., 2005). The cells were maintained in DMEM-F12 media with B27® serum-free supplement. Human pulmonary artery smooth muscle cells (HPASMC) were obtained from Invitrogen Life Technologies and were maintained in DMEM-F12 with Smooth Muscle Growth Supplement (SMGS). Cells were cultured at 37°C in a humidified atmosphere with 5% CO_2.

ID3 overexpressing endothelial cells

The HCMEC/D3 cells were transduced with either Precision LentiORF for ID3 (Thermo Scientific Open Biosystems) or empty vector lentiviral pLEX-JRED/TurboGFP by the trans-lentiviral packaging kit with Express-in transfection reagent according to the manufacturer's instructions. We used the MOI (multiplicity of infection) of 25 and selected cells that overexpressed ID3 with blasticidin S (5μg/ml) as per manufacturer's instructions. Cells expressing TurboGFP were identified by fluorescence microscopy. Using this method, we

cultured for 6 passages to generate a stable endothelial clone that overexpressed ID3 and named it EC $^{ID3+}$.

Fluorescence activated cell sorting (FACS)

After the staining, the cells were washed twice with stain buffer (BD Pharmingen) and analyzed using a Guava easyCyte flow cytometer (Millipore). For staining, 1×10^6 cells of either EC ^{wt} or EC $^{ID3+}$, were pelleted and incubated for 45 min at 4°C with the following antibodies: CD34-PE (BD Pharmingen, 581), CD133 FITC (eBioscience, 13A4) and biotin-FITC (Miltenyi Biotec), biotin conjugated VEGFR3 (eBioscience, AFL4). For cell cycle analysis, cells were harvested, rinsed with PBS, and fixed in suspension in 73% ethanol for 20 h at −20°C. After incubation at −20°C, the cells were washed with PBS containing 1% BSA, stained with PI (10 μg/ml) in PBS containing RNase A (250 μg/ml), and incubated at 37°C for 30 min in the dark before FACS analysis. Cell cycle distribution was analyzed with the Guava easyCyte™ using the CytoSoft software program according to the manufacturer's instructions. The percent DNA content was determined by FACS analysis using PI staining.

Immunohistochemistry

For immunostaining cells were blocked with 3% normal goat serum at 4°C for 1h and then incubated with antibodies: anti-ID3 (Santa Cruz Biotechnology 2B11, SC-56712), anti-VEGFR3 (Santa Cruz Biotechnology M-20, SC-637), or anti-Pyk2 (Santa Cruz Biotechnology C-19, SC-1515) overnight at 4°C. After washing with 1X PBS, cells were incubated with anti-mouse-IgG Alexa Fluor® 633 for ID3, anti-goat -IgG Alexa Fluor® 488 for Pyk2, and anti-rabbit -IgG – Alexa Fluor® 546 for VEGFR3, for 2 h. Cells were washed with PBS and then placed on cover slips with Fluoromount-G™ slide mounting medium (Electron Microscopy Science, Hatfield, PA). For immunofluorescence studies of Oct-4 and Sox-2, cells were treated with SU5416. Next, magnetic-activated cell sorted (MACS) $CD31^+$ cells were treated with SU5416 [5μM] treatment and grown in chamber slides for four days. For immunostaining cells were blocked with 3% normal goat serum at 4°C for 1h and then incubated with antibodies: anti-CD31 (Santa Cruz Biotechnology, PECAM-1, H-3, SC-37664), anti Oct-4 (Cell Signaling Technology, 2750S), or anti Sox-2 (Santa Cruz Biotechnology Y-17, SC-17320) overnight at 4°C. After washing with 1X PBS, cells were incubated with anti-mouse-IgG Alexa Fluor® 633 for CD31, anti-goat -IgG Alexa Fluor® 488 for Sox-2 and anti-rabbit-IgG Alexa Fluor® 546 for Oct-4 for 2h. Cells were washed with PBS mounted with Fluoromount-G™ reagent. For immunofluoresence of spheroids, approximately 100 spheres were fixed with 4% paraformaldehyde in 1% Triton X-100, washed in PBS, serially dehydrated in methanol (25%, 50%, 75%, 95% & 100%). Then spheroids were rehydrated in descending percentage of methanol and washed in PBS. Spheroids were incubated in 3% normal goat serum (Vector Lab, Burlingame, CA) at 4°C for 24h and washed in PBS with 0.5% Tween 20 (PBST). Next, spheroids were incubated with primary antibodies anti-Sox-2 (Santa Cruz Biotechnology Y-17, SC-17320), and anti-Oct-4 (Cell Signaling Technology, 2750S) for 48h at 4°C, washed in PBST and incubated with anti-rabbit-IgG Alexa Fluor® 546 for Oct-4 and anti-goat-IgG Alexa Fluor® 488 for Sox-2. Spheres were mounted in chamber slides and fluorescence staining analyzed. All samples were analyzed using a Nikon C1 laser scanning confocal microscope.

Immunofluorescence of ID3, CD34, αSMA, CD31, Oct4, or Sox2 positive cells was semi-quantitatively evaluated by assigning a score for the intensity of the immunofluorescence (IF) and for the proportion of cells immunostained. The product of these two values was taken to give the overall IF (total score). The intensity of the immunofluorescence (intensity score) was stratified into four categories: 0, no IF; 1, weak IF; 2, moderate IF; and 3, strong IF. Higher than 1 IF was considered positive for ID3, CD34, αSMA, CD31, Oct4, or Sox2 in cells. We counted 100 immunofluorescent cells in each group. In control, cells that were scored 1 IF were counted and expressed as a percentage. In SU5416 group, cells that were scored 2 IF and 3 IF were counted and expressed as a percentage.

Cell differentiation

The EC $^{ID3+}$ clone was grown for 7d in DMEM-F12 media with B27® serum-free supplement in ultra-low attachment plates followed by 3 days in culture media (DMEMF12 plus 5% FBS). This procedure was repeated 6 times for a total of 60 days under these conditions. Afterwards, EC $^{ID3+}$ stem-like cells were maintained in culture media for 28 days in the control group. For differentiation, EC $^{ID3+}$ stem-like cells were cultured in either SMGS plus DMEM-F12 or neurobasal media plus nerve growth factor-7S (Sigma), Glutamax, and N2 supplement for a total of 28 days. Cells were grown in LabTek(R) II 8 chambered #1.5 German coverglass system, NUNC (Thermo Fisher Scientific Inc.). We determined cell differentiation at days 7, 14, and 28 with antibodies-CD34 (control); α-smooth muscle actin (smooth muscle marker); and β-tubulin III (neuron marker). Nuclei were counterstained with DRAQ5® (Cell Signaling).

Western blotting

Whole cell lysates were prepared with lysis buffer containing [25 mM Tris-HCl buffer (pH 8.0), 150mM NaCl, 0.2% NP-40, 10% glycerol, 8 mM β-glycerophosphate, 2.5 mM sodium pyrophosphate, 10 mM NaF, 0.2 mM Na_3VO_4, 1 mM DTT and 10 μl/ml protease inhibitor cocktail (Sigma Aldrich). Proteins were quantified using the Bradford Assay Reagent (Bio-Rad) according to the manufacturer's instructions. Proteins (35–75 μg) were separated by 10% SDS-PAGE and transferred to polyvinylidene fluoride (PVDF) membranes (Millipore). Membranes were blocked with 5% nonfat milk and incubated with the following antibodies: ID3 (Cal BioReagent), CD34 (Santa Cruz Biotechnology), and VEGFR3 (Santa Cruz Biotechnology). Membranes were then incubated with horseradish peroxidase-conjugated secondary IgG antibodies and visualized with ECL Plus Western blot reagents (GE Healthcare, Amersham). The membranes were re-probed for β-actin as loading control. Electrochemiluminescence (ECL) intensity of detected target proteins was imaged and quantified with a Bio-Rad Versa Doc instrument. All immunoblots were completed a minimum of three times for each experiment.

Endothelial spheroid and 3-D cell culture

Cells used for sphere assay were first magnetic-activated cell sorted (MACS) $CD31^+$ endothelial cells. In brief, ECs were isolated using the Dynal MPC®-L Magnetic Particle Concentrator (Invitrogen Dynal AS, Oslo, Norway) and anti-CD31 conjugated magnetic Dynabeads® (Invitrogen Dynal AS) according to the manufacture's protocols. Concentrated CD31-positive ECs were suspended in serum-free stem cell medium containing DMEM/F12

(1:1) supplemented with B27®. For EC spheroid generation, approximately 100–150 cells per well were seeded in an ultra low-attachment 96-well plate (Corning Inc, Lowell, MA) with or without SU5416 treatment for four days. SU5416 was added on the day of cell seeding. For 3-D cell culture, equal proportions of EC and HPASMC were seeded in DMEM/F12 (1:1) containing B27® serum-free supplement. Next, EC spheroids were transferred into a cell culture insert precast with collagen matrix and reduced growth factor Matrigel for a 24-well plate (Corning Inc, Corning, NY). The DMEM/F12 serum-free B27® medium was carefully added into the cell culture insert, placed into the 24 well plate and incubated at 37°C for 90 days. Culture medium was replenished every 15 days.

Preparation of histological tissues

The 3-D microvascular lesions were harvested after 90 days followed by routine paraffin embedding, histological processing and staining. In brief, paraffin embedded spheroid sections were placed in xylene for 10 min and then the slides were gradually re-hydrated in successive steps with ethanol (100%, 95%, 70%) and PBS, pH 7.4. Next, the slides were stained with hematoxylin solution (Mayer, Fluka Biochemika), washed with PBS, and dehydrated in methanol (25%, 50%, 75%, 95%). After 95% methanol, we stained the slides in eosin (Fisher Scientific) and immersed the slides in 95% methanol to remove excess stain followed by 100% methanol for 10 min. The stained sections were then mounted with a cover glass using Permount (Fisher Scientific).

Immunohistochemistry of 3-D microvascular lesions

Slides of tissues generated by the 3-D cell culture were histologically prepared for microscopy as described previously. For immunofluorescence imaging studies, slides were incubated with primary antibodies anti-CD34 (Santa Cruz Biotechnology C-18, SC-7045), α-SMA(Santa Cruz Biotechnology B-4, SC-53142), and anti-ID3 (Santa Cruz Biotechnology C-20, SC-490) for 12h at 4°C, washed in PBST, and incubated with anti-mouse-IgG Alexa Fluor® 633 for α-SMA, anti-goat-IgG Alexa Fluor® 488 for CD34, and anti-rabbit-IgG Alexa Fluor® 546 for ID3 for 12h. After washing, cells were mounted and samples were analyzed using a Nikon C1 laser scanning confocal microscope.

Immunohistochemistry of in vivo pulmonary vascular lesions

In vivo pulmonary arterial lesions were generated by the combination of SU5416 treatment and chronic hypoxia as described previously (Taraseviciene-Stewart et al., 2001). Lung vasculature tissues were obtained from our collaborator, Dr. Norbert F. Voelkel, MD, Professor of Pulmonary Research and Director of the Victoria Johnson Center for Obstructive Lung Diseases. The experimental protocol was approved by the Animal Care and Use Committee of the Virginia Commonwealth University, Richmond, VA. In brief, rats were given a single dose of 20 mg/kg of SU5416 on day 1 and were then exposed to 3 weeks of hypoxia as described previously (Taraseviciene-Stewart et al., 2001). Controls included vehicle alone and exposure to hypoxia. The methods for immunohistochemistry (triple labeling) of lung vascular lesions with ID3, VEGFR3, and Pyk2 are similar to what was described in the immunofluorescence cell staining section. All tissue samples were analyzed using a Nikon C1 laser scanning confocal microscope.

Statistical analyses

All statistics were performed using VassarStats statistical software (Richard Lowry, Poughkeepsie, NY, USA). One-way analysis of variance (ANOVA) was performed to detect any differences between groups. If the result of the ANOVA is significant, pair wise comparisons between the groups were made by a post-hoc test (Tukey's HSD procedure).

Results

ID3 induces a molecular stem cell-like signature in microvascular cells

Endothelial stem/progenitor cells have been reported in circulating peripheral blood while there is also evidence for endothelial stem cells that reside locally in the endothelium of the vessel wall. Given the biological significance of Id proteins for the maintenance of stemness, we asked whether overexpression of ID3 could induce a molecular stem-cell like signature in adult microvascular ECs. To address this question, adult human microvascular ECs were transduced using a MOI of 25 with either the Precision LentiORF for ID3 overexpression or control empty lentiviral vector pLEX-JRED/TurboGFP according to the manufacturer's instructions. Cells were then seeded at clonal density and selected with blasticidin S (5μg/ml).

Vascular remodeling in the lungs of patients with IPAH was reportedly associated with elevated levels of circulating $CD133^+$ $CD34^+$ stem cell-like endothelial progenitor cells. To determine whether EC $^{ID3+}$ acquire a molecular stem cell like signature, we performed flow cytometry. We first determined the effect of ID3 on the cell surface expression of stem cell marker CD133 in cells that were positive for endothelial marker CD34 by two color flow cytometry. Figure 1A is a representative flow cytometry data analysis of EC ^{wt} and EC $^{ID3+}$, respectively. In the ID3 overexpressing cells, we observed that approximately 36% of the total cell population was positive for stem-cell markers CD133 and CD34 compared to only 5% in the wild-type cell population (Fig. 1C). This increase in $CD133^+$ $CD34^+$ cells in the EC $^{ID3+}$ population was statistically significant. Currently, there is no agreement about which combination of cell surface markers (i.e. $CD133^+$ $VEGFR2^+$ $CD34^+$) best identify a population of endothelial stem cell-like cells. Human $CD133^+$ $CD34^+$ cells that also express VEGFR3 were reported to constitute a phenotypically and functionally distinct population of endothelial stem cells (Salven et al., 2003). Therefore, we determined VEGFR3 expression in EC $^{ID3+}$ (Fig. 1B). As shown in Fig. 1D, we observed that approximately 36% of the total EC $^{ID3+}$ population was positive for endothelial stem markers VEGFR3 and CD34 compared to only 7% in wild-type cells (Fig. 1D). The increase in $VEGFR3^+$ $CD34^+$ cells in the EC $^{ID3+}$ population was statistically significant. Taken together these results show a significant $CD133^+$ $VEGFR3^+$ $CD34^+$ — molecular stem cell-like signature in the EC $^{ID3+}$ population.

As stem cells mature, they spend less time in G_0/G_1 phase due to a more robust proliferative ability as they move toward terminal differentiation. Proliferative quiescence is a state observed in stem cells which reside longer in the G_0/G_1 phase of the cell cycle; and it has been hypothesized that quiescence may prevent against the depletion of the stem cell population. Since ID3 is a known inhibitor of differentiation, we postulated that EC $^{ID3+}$

may show increased proliferative quiescence. Therefore, we asked the question of whether ID3 increased the number of cells distributed in the G_0/G_1 phase of the cell cycle as a biological indicator of proliferative quiescence. In Fig. 2A, FACS data shown are representative histograms from three independent experiments showing the effect of ID3 overexpression compared to wild-type ECs. Our flow cytometery experiments revealed that approximately 71% of the DNA content in EC $^{ID3+}$ resided in the G_0/G_1 phase compared to only 58% of the wild-type cells. Thus, EC $^{ID3+}$ showed a statistically significant 1.2-fold increase in G_0/G_1 phase cells (Fig. 2B). The percentage of DNA content in S phase decreased from approximately 11% in EC ^{wt} to 6% in EC $^{ID3+}$. Thus, ID3 significantly reduced the number of cells in S phase by more than 0.5-fold (Fig. 2B). The EC $^{ID3+}$ also showed a similar decrease in % DNA content in G_2/M phase from approximately 9% in wild-type cells to 5% in the EC $^{ID3+}$ population (Fig. 2B). Our data suggest that in the EC $^{ID3+}$ population there is a significant increase in the number of cells that reside in the G_0/G_1 phase which is indicative of proliferative quiescence. Since a higher proliferative capacity may exhaust a stem cell population, this observed increase in G_0/G_1 phase by EC $^{ID3+}$ may help to maintain a stem cell-like state by slowing cell cycle progression.

Microvascular cells treated with SU5416 show positive protein expression of ID3 and VEGFR3

The formation of microvascular lesions has been extensively studied using the SU5416/chronic hypoxia (SuHx) rodent model of severe PAH (Taraseviciene-Stewart et al., 2001; Oka et al., 2007). A chemical antagonist of VEGFR1 and 2, SU5416, has been implicated in the growth of pulmonary endothelial lesions by expanding surviving $CD34^+$ stem cell-like cells *in vitro*. Whether SU5416 treatment can lead to the expression of a molecular stem cell-like signature just as we observed in the EC $^{ID3+}$ has not been reported. Furthermore, it has not been determined whether VEGFR1/2 blockade by SU5416 treatment may actually increase the expression of other VEGF receptor family members (Nicolls et al., 2012). We have previously shown increased VEGFR3 expression in $CD34^+$ cells from EC $^{ID3+}$ population (Fig. 1B). Since SU5416 treatment is suspected of expanding a $CD34^+$ stem cell-like population which could participate in the formation of the pulmonary microvascular lesions found in the SuHx rodent model of severe PAH, we determined whether SU5416 treatment would increase VEGFR3 expression in EC ^{wt}. The wild-type ECs were treated with SU5416 [3μM] for 3h. As shown in the representative immunofluorescent images (Fig. 3A), SU5416 treatment increased both VEGFR3 and ID3 expression when compared to the vehicle control cells. SU5416 treatment showed a statistically significant increase in both $VEGFR3^+$ and $ID3^+$ immunostained cells of approximately 65% and 44%, respectively, compared to less than 5% in the vehicle control. Next, we confirmed the results from the immunofluorescent experiments by measuring the protein levels of ID3, VEGFR3, and CD34 induced by SU5416 treatment. Western blots showed that SU5416 treatment increased the relative ratio of ID3 greater than 5-fold and VEGFR3 greater than 15-fold compared to control (Fig. 3C). Our results also showed an approximate 10-fold increase in the protein level of endothelial marker CD34. We find it interesting that SU5416 chronic treatment had been previously reported to provide a selection pressure resulting in an increase in $CD34^+$ cell population that trans-differentiated into smooth muscle (SM)-like and neuronal-like cells. In contrast, our experiments showed that short-term exposure to

SU5416 of 3h significantly increased cellular levels of CD34; this cannot be explained by selection pressure. The increased expression of ID3, VEGFR3, and CD34 induced by SU5416 treatment aligns in a pattern of an angiogenic signaling pathway because all three proteins have been reported to be associated with new vessel formation.

Dysfunctional bone morphogenetic protein (BMP) signaling has been implicated in IPAH (Spiekerkoetter et al., 2013). We were intrigued by a study that showed BMP treatment differentially up-regulated proline rich tyrosine kinase 2 (Pyk2) in pulmonary artery cells from patients with severe IPAH compared to normal subjects (Fantozzi et al., 2005). Pyk2 is particularly abundant in lung and brain tissues; and Pyk2 kinase activity is reported to control pulmonary vascular EC spreading, migration, morphogenesis, as well as pulmonary vein and artery angiogenesis *ex vivo*. Therefore, the next set of experiments addressed the question of whether Pyk2 expression was also affected by exposure to SU5416. As shown in Fig. 3A, SU5416 treated EC ^{wt} showed an increased number of cells that immunostained Pyk2^{+} to approximately 70% (Fig. 3B). This increase in Pyk2 expression by SU5416 in the human ECs may help to bridge a mechanistic signaling link between the previously reported abnormal Pyk2 up-regulation observed in the cultured ECs of IPAH patients and the well-established SuHx animal model of PAH.

Microvascular cells treated with SU5416 express pluripotent transcription factors Oct-4 and Sox-2

Exposure to SU5416 has been shown to select for cells that express the stem cell marker CD34 that were differentiated into SM-like and neuronal-like cells (Sakao et al., 2007). Our present experiments showed increased ID3 expression from SU5416 treatment (Fig. 3C) and we suspect that SU5416 may contribute to stemness by modulating pluripotent transcription regulators such as ID3. The continuous expression of Oct-4 and Sox-2 in fetal ECs has been reported to induce pluripotency. More recently we have identified increased Oct-4^{+} cells within pulmonary microvascular lesions and the surroundings of remodeled vessels at 7 weeks in the SU5416 treated rodent model of PAH. Consequently, next we determined whether exposure to SU5416 could elicit the expression of Oct-4 and Sox-2 in human microvascular ECs as we previously observed with ID3. EC ^{wt} was treated with SU5416 [5μM] for 3h and then cultured in fresh media for four days. In Fig. 4A, representative images of immunofluorescent stained Oct-4^{+} and Sox-2^{+} EC ^{wt} showed that SU5416 treatment dramatically increased the expression of these transcription factors. Approximately 90% of the EC ^{wt} treated with SU5416 were Oct-4^{+} and Sox-2^{+} compared to vehicle control which was statistically significant (Fig. 4B). In addition, the cells stained 90% positive for CD31 which is a known marker found in EC stem cell-like cells (Fig. 4B). Interestingly, our data showed that SU5416 exposure resulted in a robust expression of pluripotency characterizing factors at day 4 even while the cells had only been exposed to the VEGFR blocker for 3h. One possible explanation for the long-lasting induction of these molecules by a 3h chemical exposure is that ECs concentrate SU5416. For example, a 2h exposure to 4 μM of SU5416 has been shown to produce an intracellular concentration of 450 μM in the HUVEC cell line (Mendel et al., 2000). Thus, the sustained induction of Oct-4^{+} and Sox-2^{+} expression following an acute exposure is likely the result of the SU5416 being retained in ECs even when it has been removed from the culture medium.

Sphere-forming assays are widely used in stem cell biology to culture cells under non-adherent conditions in order to characterize stemness. Colony forming units of ECs are typically enriched in $CD34^+$ $CD133^+$ cells. Intriguingly, colony forming ECs from individuals with IPAH have been shown to produce large cell clusters and angioproliferative lesions in the Matrigel Plug xenograft model. As an alternative to our experiments in monolayer cultures (Fig. 4), we cultured ECs using a sphere forming assay in order to verify whether SU5416 induced Oct-4 and Sox-2 in a more homogeneous population of stem cell-like cells. The sphere forming assay has been widely used to select for stem cell-like cells under serum-free culture conditions. Since each sphere is derived from a single cell and therefore clonal, the more stringent cell selection conditions that arise from SU5416 treatment in conjunction with the sphere forming assay allowed us to examine an association of clonal cell growth with the stemness profile so far identified. Prior to the sphere assay, wild-type endothelial cells were enriched by magnetic-activated cell sorting for $CD31^+$ cells. Next, EC ^{wt} were seeded at clonal density and cultured as spheroids in DMEM-F12 B27® serum-free media with or without SU5416 treatment as described previously in the Materials and Methods Section. Diameter was measured using a total of 15 endothelial spheroids with a minimum diameter of 70μm were counted in each experimental group. Data were analyzed by ANOVA; Tukey HSD test for multiple comparisons. In Fig. 5A, immunofluorescence staining of Oct-4 and Sox-2 was significantly greater in SU5416 treated cells and confirmed our previous data of EC ^{wt} cultured as a monolayer (Fig. 4A). The EC spheroid consisted of an acellular core in the vehicle control experiments (Fig. 5A, top row) as expected when the EC ^{wt} are cultured under serum-free conditions. In clear contrast, the EC ^{wt} spheroids treated with SU5416 showed a significant growth (diameter) increase at days 2 and 4 when compared to vehicle controls (Fig 5B). Unlike the previous studies where SU5416 treatment of EC ^{wt} grown as a monolayer selected for a $CD34^+$ endothelial stem cell-like population, the sphere forming assay under serum-free conditions selects for a VEGFR blockade-triggered homogeneous population of stem cell-like cells. This is an important novel finding. The observed increase in spheroid diameter correlated with a robust expression of Oct-4 and Sox-2. Taken together, our findings suggest that SU5416 exposure may not only expand a population of $CD34^+$ endothelial stem cell-like cells as a consequence of VEGFR1 and 2 blockade, but additionally or alternatively activate biological pathways that increase the expression of pluripotent signaling molecules. Chemical-induced reprogramming has been shown by others to be a novel approach to generate pluripotent stem cells (Li et al., 2011). Whereas the continuous expression of ID3 and Oct-4 can reprogram mouse embryonic fibroblasts into neural stem cells (Moon et al., 2012), the chemical induction of pluripotent transcription factors in adult human microvascular ECs by SU5416 treatment under conditions of the sphere assay has not been previously reported. This result leads us to postulate that SU5416 exposure may contribute to the growth of stem cell-like cells by inducing pluripotent factors: ID3, Oct-4, and Sox-2.

EC $^{ID3+}$ stem-like cells display a pluripotent morphology

Since our previous data showed that ID3 induced a molecular stem cell-like signature, we further determined whether the EC $^{ID3+}$ clone was morphologically pluripotent. To determine pluripotency, we generated EC $^{ID3+}$ stem-like cells as described in the *Materials & Methods* section. Next, the EC $^{ID3+}$ stem-like cells were seeded in monolayer and cultured

with either neuronal or smooth muscle differentiation medium. At 7 days the EC $^{ID3+}$ stem-like cells were assessed by phase-contrast microscopy for morphological changes. As shown in Fig. 6A, the untreated EC $^{ID3+}$ stem-like cells appeared as a monolayer of cuboidal, broad, flat cells. After 7 day treatment with smooth muscle differentiation medium, the stem-like ECs began to show a heterogeneous phenotype of both cuboidal cells as well as the characteristic elongated spindle shape of a VSMC (Fig. 6A). Likewise after neuronal induction, EC $^{ID3+}$ stem-like cells displayed changes in morphology including shrinkage of cytoplasm, formation of axon— and dendrite—like cytoplasmic projections (Fig. 6A). Cell differentiation markers were determined using immunofluorescence at days 7, 14, and 28. For immunofluorescence imaging studies, slides were incubated with primary antibodies anti-CD34, α-smooth muscle actin (α-SMA), and β-tubulin III. As shown in Fig. 6B, smooth muscle-like cells immunostained positive for the α-SMA; and negative for both neuronal marker β-tubulin III and endothelial stem cell marker CD34. The immunofluorescence images indicated that these cells persisted to show an elongated spindle shape beyond 7 days. Furthermore, we observed the following morphological changes of a shrinking cytoplasm and a more rounded nuclei compared to the untreated EC $^{ID3+}$ stem-like cells. As shown in Fig 6B, neuronal-like cells immunostained positive for neuronal marker β-tubulin III; and negative for both markers CD34 and α-SMA. Immunofluorescence images of neuronal differentiation (Fig. 6B) showed that the cytoplasm of EC $^{ID3+}$ stem-like cells began to retract toward the nucleus, forming contracted cell bodies with extended cytoplasmic extensions. Beyond 7 days, the EC $^{ID3+}$ stem-like cells treated with neuronal differentiation media continued to form contracted cell bodies with extended cytoplasmic extensions. These extensions morphologically resembled axon— and dendrite—like processes up to 28 days. Although these histological changes consistent with smooth muscle and neuronal differentiation were seen in EC $^{ID3+}$ stem-like cells, they do not show that these cells are, in fact, functional SMCs or neurons. These results however do confirm that the EC $^{ID3+}$ stem-like cells are morphologically pluripotent under these specific conditions.

EC $^{ID3+}$ stem-like cells form a 3-D microvascular lesion

Based on the morphological pluripotency of EC $^{ID3+}$ stem-like cells, we postulate that these endothelial stem-like cells may serve as a human model system for studying microvascular lesions. Our FACS analysis of EC $^{ID3+}$ indicated that overexpression of ID3 increased the levels of VEGFR3. Interestingly, VEGFR3 is reported to be highly expressed on glioma tumor endothelium (Grau et al., 2007); and we recently communicated that VEGFR3 signaling contributes to angioobliterative pulmonary hypertension (*communicated*, *Ayers et al. Pulmonary Circulation*). Taken together, this data is consistent with the hypothesis that EC $^{ID3+}$ stem-like cells have utility in the study of microvascular lesions involved in other pathologies such as pulmonary plexiform lesions. For instance, morphologically and immunohistochemically, the plexiform lesion present in severe pulmonary hypertension was reported to resemble the neovascularization associated with the brain tumor glioblastoma multiform (Tuder et al., 1994a). To determine whether EC $^{ID3+}$ stem-like cells may serve as a human model of microvascular lesions, we cultured EC $^{ID3+}$ stem-like cells with pulmonary arterial SMCs to mimic an *in vitro* 3-D pulmonary microvascular lesion.

Cell culture assays that stimulate the differentiation of ECs into capillary-like tubes are usually performed on 3-D matrices consisting of fibrin, collagen or Matrigel that mimic the *in vivo* environment. Based on our previous findings that showed ID3 overexpression significantly increased a molecular stem cell-like signature of $CD133^+$ $VEGFR3^+$ $CD34^+$, we evaluated the differentiation capacity of these cells when cultured with pulmonary arterial SMCs using a modified 3-D culture protocol (Kalabis et al., 2012). Figure 7A shows a diagrammatic representation of the protocol used to prepare the 3-D microvascular lesions. Briefly, equal proportions of cells from either EC ^{wt} or EC $^{ID3+}$ were seeded with SMCs in serum-free B27® supplemented DMEM-F12. After formation of EC/SMC spheroids, the spheroids were transferred into pre-cast collagen matrix and Matrigel containing transwell inserts. Next, serum-free DMEM-F12 supplemented with B27® was used to fill transwell carriers containing the inserts and incubated at 37°C for 90 days with a fresh change of medium every 15 days. After allowing the EC/SMC spheroids to self-organize and grow for 90 days, 3-D cell cultures were harvested and processed using routine paraffin embedding and histological staining techniques. Under these conditions spheroids cultured with EC ^{wt} did not survive for more than 15 days and there was no tube formation (data not shown). However, spheroids containing cells from the EC $^{ID3+}$ developed capillary-like structures. Figure 7B shows a representative phase photograph of a tube-like structure (blue arrow) connected to a spheroid (red arrow). The number of tube structures in EC $^{ID3+}$/SMC spheroids gradually increased during the 90 day time period as shown in Fig. 7C. Although the EC ^{wt}/SMC culture did not survive to form spheroids, our data suggest that ID3 may give ECs an advantage in surviving serum-free 3-D culture. If EC spheroids are not exposed to growth factors such as in our serum-free conditions, it has been demonstrated that the center cells undergo apoptosis leaving an EC spheroid consisting of an acellular core (Korff et al., 1998). This may explain why the EC ^{wt} did not survive as they were not in a proliferative quiescent state and relied heavily on growth factors. Upon histological examination, the tube-like structures showed a well-defined and robust cord (Fig. 7D). The small circular morphology of the ECs are indicated by the green arrow while the bigger spindle shaped SMCs are shown by the black arrow. As shown in Fig. 7E, the morphology of the 3-D microvascular lesion resembled a glomeruloid body with lumen-like structures. This cross-sectional view of the lesion showed a viable and intact cellular core from which the tube-like structures originate. The endothelial nature of tube structures as well as the contribution of SMCs was confirmed by staining for the endothelial marker CD34 and the SMC marker α-SMA. As shown in the immunofluorescence image (Fig. 7F), SMCs organized mainly along the tube-like structures while the majority of ECs composed both the spherical core as well the tube-like structures. Approximately, 45% of the cells immunostained positive for the SMC marker and 90% stained positive for the EC marker (Fig. 7G). These findings suggest that the SMCs terminally differentiated or could not proliferate in the serum-free conditions based on the initial equal cell seeding ratio of EC/SMC. Although ID3 overexpression did not prevent the differentiation of ECs into tube-like structures, our findings suggest that ID3 overexpression prevented the terminal differentiation of a core of ECs that was able to support the growth of a glomeruloid microvascular lesion and tube-like structures for the entire 90 day period. Thus, EC $^{ID3+}$ stem-like cells plus their progeny eventually outnumbered the SMCs by the end of the experiment. Our results show that under these culture conditions, EC $^{ID3+}$ stem-like cells

can form a 3-D microvascular lesion that morphologically resemble glomeruloid microvascular lesions that have been reported in glioblastoma multiform and plexiform lesions of IPAH.

In vivo pulmonary vascular lesions overexpress ID3, VEGFR3, Pyk2

Our previous experiments with SU5416 treated EC ^{wt} showed a significant increase in the expression levels of ID3, VEGFR3, and Pyk2. SU5416 treatment plus chronic hypoxia of rodents is a well-known model of severe PAH that produces plexiform lesions that closely resemble those found in humans (Taraseviciene-Stewart et al., 2001). To determine whether formation of pulmonary vascular lesions caused by SU5416 plus chronic hypoxia treatment in rodents affected the level of these markers, we performed immunohistochemistry on lung tissue from rodents using antibodies for ID3, VEGFR3, and Pyk2. As shown in Fig. 8A, the cells that line the lumen of the pulmonary artery in both the vehicle control and the chronic hypoxia groups form a uniform monolayer. In contrast, the cells lining the lumen from the SU5416-treated lung exposed to chronic hypoxia for 3 wk were piled on top of each other leading to lumen obliteration. In the endothelial lesions from the SuHx treated lungs, we observed that approximately 80% of the cells expressed ID3, VEGFR3, and Pyk2 compared to only 10% of the cells in the control animals. In the 3 week chronic hypoxia group, we observed that approximately 50% of the cells expressed all three markers. As shown in Fig. 8B, expression of all three markers was significantly higher in the SU5416 + hypoxia treatment group compared to hypoxia alone group.

Discussion

Many investigators and laboratories have made important contributions which have greatly advanced our knowledge of the cellular and molecular mechanisms which control the development of microvascular lesions (Hassoun et al., 2009); yet the investigation of stem cells and their roles in vessel remodeling is still in its infancy. Our study showed that ID3 contributes to the acquisition of a molecular stem cell-like signature in human microvascular ECs and when cultured under specific conditions EC $^{ID3+}$ stem-like cells formed a 3-D microvascular lesion that morphologically resembled glomeruloid microvascular lesions known to be found in other pathologies including glioblastoma, NSCLC, and IPAH (Rojiani et al., 1996; Tanaka et al., 2003; Tuder et al., 1994a). Based on the morphological pluripotency of EC $^{ID3+}$ stem-like cells, we postulate that these endothelial stem-like cells may serve as a human model system for studying microvascular lesions. In this study, we compared the following endothelial types EC ^{wt} and EC $^{ID3+}$ and determined the effects of ID3 overexpression or exposure to SU5416— a chemical inducer of microvascular lesions had on the molecular stemness signature. The major findings of our investigations are: (i) continuous expression of ID3 produced a molecular EC stemness signature consisting of CD133^{+} VEGFR3^{+} CD34^{+} cells; (ii) EC ^{wt} exposed to the VEGFR1/2 inhibitor—SU5416 showed positive protein expression of ID3, VEGFR3, CD34; (iii) EC ^{wt} exposed to SU5416 showed increased expression of pluripotent transcription regulators ID3, Oct-4, and Sox-2; (iv) EC $^{ID3+}$ stem-like cells supported the formation of a 3-D microvascular lesion co-cultured with SMCs; and (v) *in vivo* microvascular lesions induced by SU5416 plus chronic

hypoxia in rodents showed an increased expression of ID3, VEGFR3, and Pyk2 similar to exposed EC ^{wt}.

Given the biological significance of Id proteins in stemness, we asked whether overexpression of ID3 would produce in ECs a molecular signature of stemness. In our studies we showed that either continuous ID3 overexpression or SU5416 treatment altered the levels of stemness markers in ECs. Our data show that ID3 lead to the expression of $CD133^+$ $CD34^+$ cells that also express VEGFR3, a molecular signature previously reported to identify endothelial stem cells (Salven et al., 2003). Our results also illustrate that the expression of the pluripotent transcription regulators ID3, Oct-4, and Sox-2 may be novel molecular targets of SU5416. This finding is significant in that it points toward a potential mechanism of chemical-induced stemness in not only the SuHx model of microvascular lesion formation, but also towards the role of environmental exposures in re-programming vascular cells to a more stem cell-like state. In support of this idea, others have already shown that the continuous expression of ID3 and Oct-4 de-differentiated mouse embryonic fibroblasts into neural stem cells (Moon et al., 2012). Our study lends support for the role of ID3 in stemness as demonstrated with EC $^{ID3+}$ morphologically differentiated into neuronal — and smooth muscle—like cells. Our results show that EC ^{wt} exposed to SU5416 had increased expression of transcriptional regulators ID3, Oct-4, and Sox-2. As mentioned earlier SU5416 has been reported to expand a population of stem-like cells in the formation of microvascular lesions; however, our findings are novel in that we show pluripotent transcription factors and stemness markers expressed within only 3h of chemical exposure in human vascular cells. SU5416 exposure appears to directly alter biological pathways that increase the expression of pluripotent signaling molecules in addition to or alternatively to the expansion of an existing population of vascular stem cells.

Our findings indicate that EC $^{ID3+}$ stem-like cells may serve as a human model of microvascular lesions. In this study, we showed similarities in the molecular signature shared between an *in vitro* 3-D human microvascular lesion formed from EC $^{ID3+}$/PASMC cell culture and *in vivo* microvascular lesions from a rodent model of severe PAH. It is probable that several cell types and perhaps several precursor and stem cells contribute to the angioobliterative remodeling in PAH. Yet because of the early emphasis on exuberant EC growth in idiopathic PAH and the concept that “primitive angioformative cell commit to differentiate into endothelial cells” (Tuder et al., 1994b) we have postulated on ECs as one cell of origin of microvascular lesions because EC stem-like cells can be involved in repairing vascular injury. Using a novel 3-D, we demonstrated that ID3 was essential for EC stability and 3-D microvascular lesion formation. The EC $^{ID3+}$ sustained the growth of glomeruloid microvascular lesions in a 3-D cell culture model for up to 90 days, however, it is unclear how ID3 overexpression sustained the prolonged growth of this vascular lesion. Cell cycle analysis revealed that EC $^{ID3+}$ resided more in the G_0/G_1 phase and because a higher proliferative capacity may exhaust the stem cell population, our observed increase in G_0/G_1 phase by ID3— thus may help to support our concept of stemness by slowing cell cycle progression down. Although we used the EC $^{ID3+}$ stem-like cells to model pulmonary microvascular lesions, the significance of using EC with a stem cell-like molecular signature is in its application to study other pathological processes associated with the microvascular

lesion formation. Furthermore, this model may allow for studying the early processes involved in the development of the vascular lesion.

A large number of environmental factors can potentially influence and de-regulate reactive oxygen species (ROS) mediated signaling which may contribute to abnormal vascular development or de-differentiation. We hypothesize that switch in the molecular stemness profile of ECs may occur during the development of angioproliferative lesions found in severe forms of PAH. Based on our EC culture data we expected to see an increase in VEGFR3 expression (a marker of endothelial stem-like cells) in microvascular lesions of the SuHx model, but not an increase in its expression due to hypoxia alone. VEGFR3 activation by ROS has been reported to promote survival of ECs exposed to oxidative stress (Wang et al., 2004), and it may be a response to oxidative stress that led to the observed increase in VEGFR3 expression of rats exposed to hypoxia alone. Importantly, SU5416-induced expression of ID3, VEGFR3, and Pyk2 occurred both *in vitro* in the human cells and the rat microvascular lesions. A detailed exploration of the mechanisms whereby these molecules participate in vascular lesion formation will be necessary. Activation of VEGFR3 leads to the phosphorylation of Pyk2 which is involved in the coordination of cell growth (Liu et al., 1997). ID3 and Pyk2 are redox sensitive molecules and an increase in their individual expression could be due to oxidative stress that is already known to be generated during the 3wk chronic hypoxia treatment (Hoshikawa et al., 2001). Several lines of evidence support this observation. The non-receptor protein tyrosine kinase Pyk2 is activated by ROS in vascular cells while redox signaling has been shown to control ID3 gene expression and protein phosphorylation (Frank et al., 2000; Mueller et al., 2002; Felty et al., 2008). Since other non-receptor tyrosine kinases have already been shown to regulate Id expression (Gautschi et al., 2008), we postulate that ID3 may be a novel target of Pyk2 signaling that is triggered by oxidative stress. Thus, reprogramming of ECs to stem-like cells may be regulated in part by a redox sensitive VEGFR3→Pyk2→ID3 signaling pathway.

In conclusion, ID3 contributes to the acquisition of a molecular stem cell-like signature—$CD133^+$ $VEGFR3^+$ $CD34^+$ in human microvascular ECs. Furthermore, under defined cell culture conditions EC $^{ID3+}$ stem-like cells formed a 3-D vascular tissue that morphologically resembled glomeruloid microvascular lesions. We demonstrated similarities in the molecular stem cell-like signature shared between an *in vitro* 3-D human microvascular lesion formed from EC $^{ID3+}$/PASMC cell culture and *in vivo* microvascular lesions from a rodent model of severe PAH. Understanding how normal and stem-like cells utilize ID3 may open up new avenues for a better understanding of the molecular mechanisms which are underlying the pathological development of microvascular lesions in diseases such as proliferative diabetic retinopathy, glioblastoma, NSCLC, and IPAH. Potential clinical implications of our data are the development of biomarkers and inhibitors of ID3 signaling in the context of treating diseases that harbor proliferative microvascular lesions. Because ID3 produces a molecular stemness signature in ECs and because EC $^{ID3+}$ stem-like cells have the capacity to form 3-D microvascular lesions, our data point towards an important role for ID3 in the development of vascular proliferative disorders.

Acknowledgments

This research is supported by grants from NIH SC3 Award (1SC3GM084827-01A1). We would also like to thank Dr. Elena Kaftanovskaya, FIU Department of Human and Molecular Genetics, for her professional expertise and kind help with our histology sample preparation.

References

Chow K, Fessel JP, Kaoriihida S, Schmidt EP, Gaskill C, Alvarez D, Graham B, Harrison DG, Wagner DH Jr, Nozik-Grayck E, West JD, Klemm DJ, Majka SM. Dysfunctional resident lung mesenchymal stem cells contribute to pulmonary microvascular remodeling. Pulm Circ. 2013; 3:31–49. [PubMed: 23662173]

Diller GP, Thum T, Wilkins MR, Wharton J. Endothelial progenitor cells in pulmonary arterial hypertension. Trends Cardiovasc Med. 2010; 20:22–29. [PubMed: 20685574]

Fantozzi I, Huang W, Zhang J, Zhang S, Platoshyn O, Remillard CV, Thistlethwaite PA, Yuan JX. Divergent effects of BMP-2 on gene expression in pulmonary artery smooth muscle cells from normal subjects and patients with idiopathic pulmonary arterial hypertension. Exp Lung Res. 2005; 31:783–806. [PubMed: 16368652]

Felty Q, Porther N. Estrogen-induced redox sensitive Id3 signaling controls the growth of vascular cells. Atherosclerosis. 2008; 198:12–21. [PubMed: 18281048]

Frank GD, Motley ED, Inagami T, Eguchi S. PYK2/CAKbeta represents a redox-sensitive tyrosine kinase in vascular smooth muscle cells. Biochem Biophys Res Commun. 2000; 270:761–765. [PubMed: 10772898]

Gambaryan N, Perros F, Montani D, Cohen-Kaminsky S, Mazmanian M, Renaud JF, Simonneau G, Lombet A, Humbert M. Targeting of c-kit+ haematopoietic progenitor cells prevents hypoxic pulmonary hypertension. Eur Respir J. 2011; 37:1392–1399. [PubMed: 20884740]

Gautschi O, Tepper CG, Purnell PR, Izumiya Y, Evans CP, Green TP, Desprez PY, Lara PN, Gandara DR, Mack PC, Kung HJ. Regulation of Id1 expression by SRC: implications for targeting of the bone morphogenetic protein pathway in cancer. Cancer Res. 2008; 68:2250–2258. [PubMed: 18381431]

Grau SJ, Trillsch F, Herms J, Thon N, Nelson PJ, Tonn JC, Goldbrunner R. Expression of VEGFR3 in glioma endothelium correlates with tumor grade. J Neurooncol. 2007; 82:141–150. [PubMed: 17115285]

Hassoun PM, Mouthon L, Barbera JA, Eddahibi S, Flores SC, Grimminger F, Jones PL, Maitland ML, Michelakis ED, Morrell NW, Newman JH, Rabinovitch M, Schermuly R, Stenmark KR, Voelkel NF, Yuan JX, Humbert M. Inflammation, growth factors, and pulmonary vascular remodeling. J Am Coll Cardiol. 2009; 54:S10–S19. [PubMed: 19555853]

Hoshikawa Y, Ono S, Suzuki S, Tanita T, Chida M, Song C, Noda M, Tabata T, Voelkel NF, Fujimura S. Generation of oxidative stress contributes to the development of pulmonary hypertension induced by hypoxia. J Appl Physiol (1985). 2001; 90:1299–1306. [PubMed: 11247927]

Jin X, Yin J, Kim SH, Sohn YW, Beck S, Lim YC, Nam DH, Choi YJ, Kim H. EGFR-AKT-Smad signaling promotes formation of glioma stem-like cells and tumor angiogenesis by ID3-driven cytokine induction. Cancer Res. 2011; 71:7125–7134. [PubMed: 21975932]

Kalabis J, Wong GS, Vega ME, Natsuizaka M, Robertson ES, Herlyn M, Nakagawa H, Rustgi AK. Isolation and characterization of mouse and human esophageal epithelial cells in 3D organotypic culture. Nat Protoc. 2012; 7:235–246. [PubMed: 22240585]

Korff T, Augustin HG. Integration of endothelial cells in multicellular spheroids prevents apoptosis and induces differentiation. J Cell Biol. 1998; 143:1341–1352. [PubMed: 9832561]

Lee SD, Shroyer KR, Markham NE, Cool CD, Voelkel NF, Tuder RM. Monoclonal endothelial cell proliferation is present in primary but not secondary pulmonary hypertension. J Clin Invest. 1998; 101:927–934. [PubMed: 9486960]

Li Y, Zhang Q, Yin X, Yang W, Du Y, Hou P, Ge J, Liu C, Zhang W, Zhang X, Wu Y, Li H, Liu K, Wu C, Song Z, Zhao Y, Shi Y, Deng H. Generation of iPSCs from mouse fibroblasts with a single gene, Oct4, and small molecules. Cell Res. 2011; 21:196–204. [PubMed: 20956998]

Liu ZY, Ganju RK, Wang JF, Schweitzer K, Weksler B, Avraham S, Groopman JE. Characterization of signal transduction pathways in human bone marrow endothelial cells. Blood. 1997; 90:2253–2259. [PubMed: 9310476]

Lowery JW, Frump AL, Anderson L, DiCarlo GE, Jones MT, de Caestecker MP. ID family protein expression and regulation in hypoxic pulmonary hypertension. Am J Physiol Regul Integr Comp Physiol. 2010; 299:R1463–R1477. [PubMed: 20881097]

Mendel DB, Schreck RE, West DC, Li G, Strawn LM, Tanciongco SS, Vasile S, Shawver LK, Cherrington JM. The angiogenesis inhibitor SU5416 has long-lasting effects on vascular endothelial growth factor receptor phosphorylation and function. Clin Cancer Res. 2000; 6:4848–4858. [PubMed: 11156244]

Moon JH, Heo JS, Kwon S, Kim J, Hwang J, Kang PJ, Kim A, Kim HO, Whang KY, Yoon BS, You S. Two-step generation of induced pluripotent stem cells from mouse fibroblasts using Id3 and Oct4. J Mol Cell Biol. 2012; 4:59–62. [PubMed: 22131360]

Mueller C, Baudler S, Welzel H, Bohm M, Nickenig G. Identification of a novel redox-sensitive gene, Id3, which mediates angiotensin II-induced cell growth. Circulation. 2002; 105:2423–2428. [PubMed: 12021231]

Nicolls MR, Mizuno S, Taraseviciene-Stewart L, Farkas L, Drake JI, Al HA, Gomez-Arroyo JG, Voelkel NF, Bogaard HJ. New models of pulmonary hypertension based on VEGF receptor blockade-induced endothelial cell apoptosis. Pulm Circ. 2012; 2:434–442. [PubMed: 23372927]

Oka M, Homma N, Taraseviciene-Stewart L, Morris KG, Kraskauskas D, Burns N, Voelkel NF, McMurtry IF. Rho kinase-mediated vasoconstriction is important in severe occlusive pulmonary arterial hypertension in rats. Circ Res. 2007; 100:923–929. [PubMed: 17332430]

Rai PR, Cool CD, King JA, Stevens T, Burns N, Winn RA, Kasper M, Voelkel NF. The cancer paradigm of severe pulmonary arterial hypertension. Am J Respir Crit Care Med. 2008; 178:558–564. [PubMed: 18556624]

Rojiani AM, Dorovini-Zis K. Glomeruloid vascular structures in glioblastoma multiforme: an immunohistochemical and ultrastructural study. J Neurosurg. 1996; 85:1078–1084. [PubMed: 8929498]

Sakao S, Taraseviciene-Stewart L, Cool CD, Tada Y, Kasahara Y, Kurosu K, Tanabe N, Takiguchi Y, Tatsumi K, Kuriyama T, Voelkel NF. VEGF-R blockade causes endothelial cell apoptosis, expansion of surviving CD34+ precursor cells and transdifferentiation to smooth muscle-like and neuronal-like cells. FASEB J. 2007; 21:3640–3652. [PubMed: 17567571]

Sakurai D, Tsuchiya N, Yamaguchi A, Okaji Y, Tsuno NH, Kobata T, Takahashi K, Tokunaga K. Crucial role of inhibitor of DNA binding/differentiation in the vascular endothelial growth factor-induced activation and angiogenic processes of human endothelial cells. J Immunol. 2004; 173:5801–5809. [PubMed: 15494533]

Salven P, Mustjoki S, Alitalo R, Alitalo K, Rafii S. VEGFR-3 and CD133 identify a population of CD34+ lymphatic/vascular endothelial precursor cells. Blood. 2003; 101:168–172. [PubMed: 12393704]

Spiekerkoetter E, Tian X, Cai J, Hopper RK, Sudheendra D, Li CG, El-Bizri N, Sawada H, Haghighat R, Chan R, Haghighat L, de JPV, Wang L, Reddy S, Zhao M, Bernstein D, Solow-Cordero DE, Beachy PA, Wandless TJ, Ten DP, Rabinovitch M. FK506 activates BMPR2, rescues endothelial dysfunction, and reverses pulmonary hypertension. J Clin Invest. 2013; 123:3600–3613. [PubMed: 23867624]

Tanaka F, Oyanagi H, Takenaka K, Ishikawa S, Yanagihara K, Miyahara R, Kawano Y, Li M, Otake Y, Wada H. Glomeruloid microvascular proliferation is superior to intratumoral microvessel density as a prognostic marker in non-small cell lung cancer. Cancer Res. 2003; 63:6791–6794. [PubMed: 14583475]

Taraseviciene-Stewart L, Kasahara Y, Alger L, Hirth P, Mc MG, Waltenberger J, Voelkel NF, Tuder RM. Inhibition of the VEGF receptor 2 combined with chronic hypoxia causes cell death-dependent pulmonary endothelial cell proliferation and severe pulmonary hypertension. FASEB J. 2001; 15:427–438. [PubMed: 11156958]

Tuder RM, Groves B, Badesch DB, Voelkel NF. Exuberant endothelial cell growth and elements of inflammation are present in plexiform lesions of pulmonary hypertension. Am J Pathol. 1994a; 144:275–285. [PubMed: 7508683]

Tuder RM, Groves B, Badesch DB, Voelkel NF. Exuberant endothelial cell growth and elements of inflammation are present in plexiform lesions of pulmonary hypertension. Am J Pathol. 1994b; 144:275–285. [PubMed: 7508683]

Tuder RM, Voelkel NF. Plexiform lesion in severe pulmonary hypertension: association with glomeruloid lesion. Am J Pathol. 2001; 159:382–383. [PubMed: 11438486]

Wang JF, Zhang X, Groopman JE. Activation of vascular endothelial growth factor receptor-3 and its downstream signaling promote cell survival under oxidative stress. J Biol Chem. 2004; 279:27088–27097. [PubMed: 15102829]

Weksler BB, Subileau EA, Perriere N, Charneau P, Holloway K, Leveque M, Tricoire-Leignel H, Nicotra A, Bourdoulous S, Turowski P, Male DK, Roux F, Greenwood J, Romero IA, Couraud PO. Blood-brain barrier-specific properties of a human adult brain endothelial cell line. FASEB J. 2005; 19:1872–1874. [PubMed: 16141364]

Yang J, Li X, Li Y, Southwood M, Ye L, Long L, Al-Lamki RS, Morrell NW. Id proteins are critical downstream effectors of BMP signaling in human pulmonary arterial smooth muscle cells. Am J Physiol Lung Cell Mol Physiol. 2013; 305:L312–L321. [PubMed: 23771884]

Highlights

- ID3 overexpression significantly increased stemness markers in endothelial cells
- ID3 overexpression resulted in vascular stem cell signature—$CD133^+$ $VEGFR3^+$ $CD34^+$
- ID3 overexpressing cell phenotype was similar to microvascular glomeruloid lesions
- VEGFR inhibitor SU5416 significantly altered stemness markers in endothelial cells

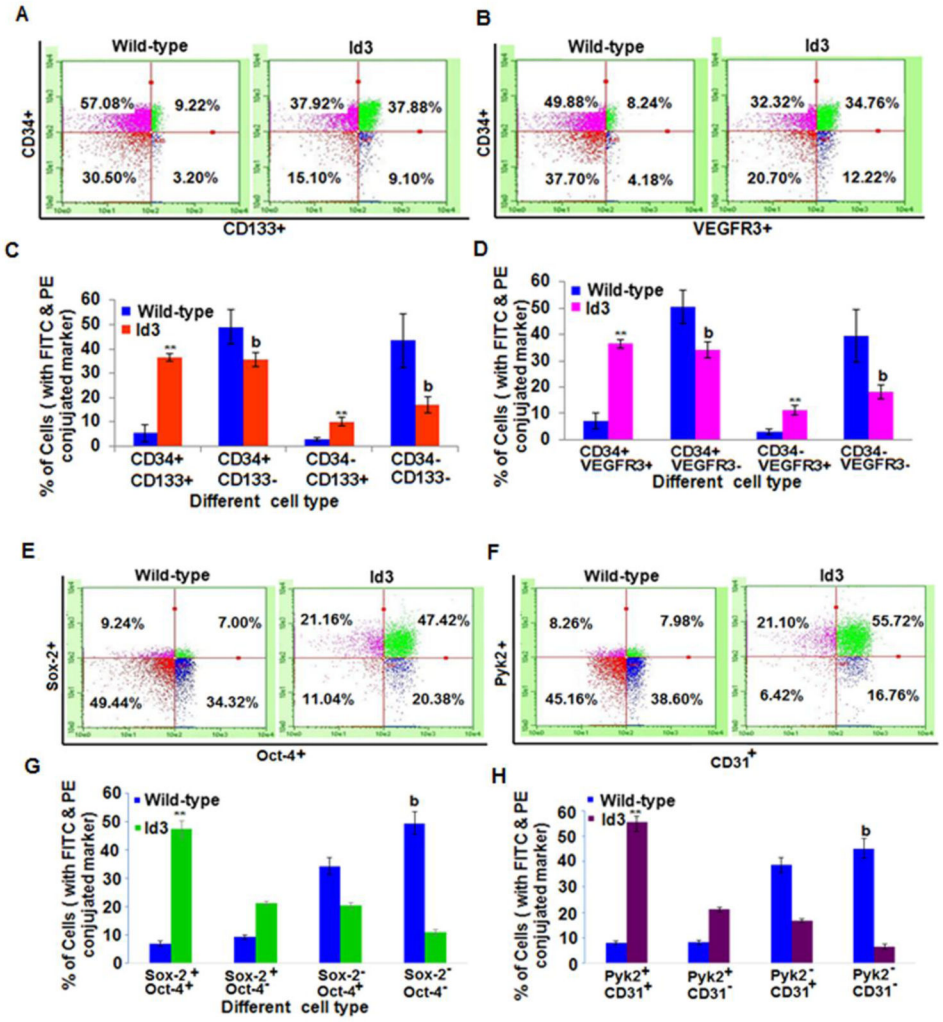

Fig. 1. Molecular endothelial stem signature induced by ID3 overexpression

Cell surface expression of endothelial stem markers CD133, VEGFR3, CD34 was analyzed by two color flow cytometry. (A) Representative flow cytometry data analysis of EC ^{wt} and EC $^{ID3+}$ analyzed for the co-expression of endothelial marker CD34 and stem marker CD133. (B) Representative flow cytometric analysis of CD34 and VEGFR3 co-expression in EC ^{wt} and EC $^{ID3+}$. (C) CD133^{+} cells were approximately 7-fold higher in EC $^{ID3+}$ compared to EC ^{wt}. Bar graph represents the flow cytometric data for CD133 and CD34 co-expression from three independent experiments ± SD. (D) VEGFR3^{+} cells were approximately 5-fold higher in EC $^{ID3+}$ compared to EC ^{wt}. (E) Representative flow cytometry data analysis of EC ^{wt} and EC $^{ID3+}$ analyzed for the co-expression of Sox2 and Oct4. (F) Representative flow cytometric analysis of CD31 and Pyk2 co-expression in EC ^{wt} and EC $^{ID3+}$. (G) Sox2 and Oct4 positive cells were approximately 6.7-fold higher in EC $^{ID3+}$ compared to EC ^{wt}. Bar graph represents the flow cytometric data for Sox2 and Oct4 co-expression from three independent experiments ± SD. (H) Pyk2 and CD31 positive cells were approximately 7-fold higher in EC $^{ID3+}$ compared to EC ^{wt}. Graph of flow cytometric data for Pyk2 and CD31 co-expression derived from three independent

experiments ± SD. Each column represents mean marker expression in either EC $^{ID3+}$ **p<0.01 vs. EC ^{wt} for increase; or EC $^{ID3+}$ ***b*** p<0.01 vs. EC ^{wt} for decrease. Data were analyzed by ANOVA; Tukey HSD test for multiple comparisons.

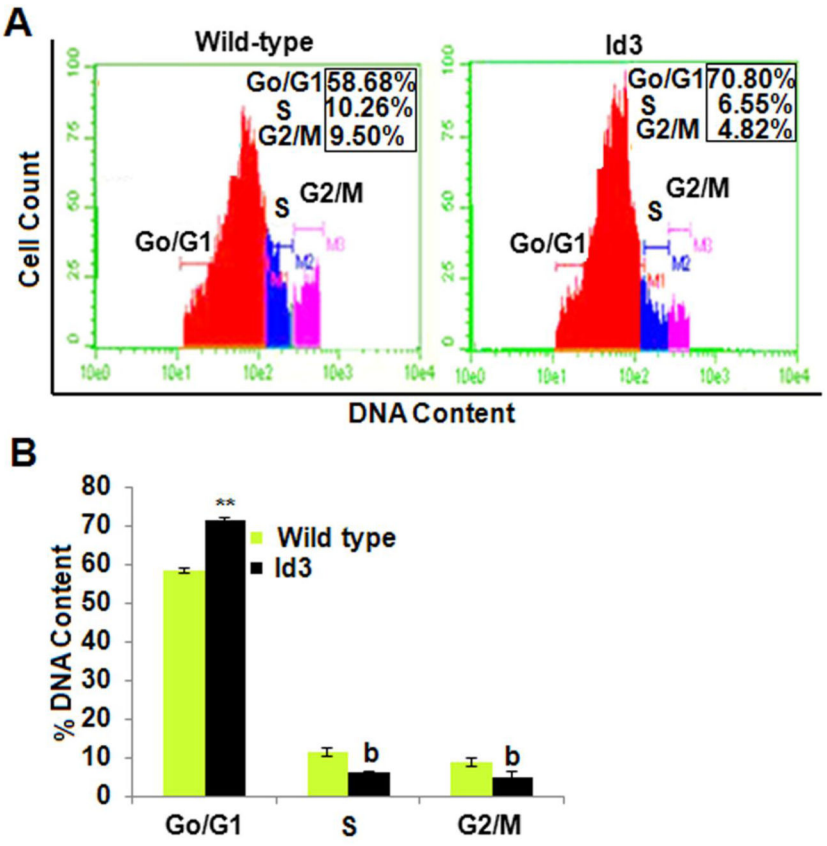

Fig. 2. Continuous ID3 expression increased the population of cells in the G_0/G_1 phas

The cell cycle distribution of EC $^{ID3+}$ compared to EC ^{wt} was determined by flow cytometry. (A) Representative flow cytometry histogram of percent DNA content distributed among the cell cycle phases based on PI fluorescence for EC ^{wt} (left panel) and EC $^{ID3+}$ (right panel). (B) EC $^{ID3+}$ showed a statistically significant 1.2-fold increase in cells residing in the G_0/G_1 phase compared to EC ^{wt}. This graph represents the mean of three independent experiments for cell cycle distribution of EC ^{wt} and EC $^{ID3+}$ ± SD. Each column represents % DNA content in cell cycle phases of either EC $^{ID3+}$ $^{**}p<0.01$ vs. EC ^{wt} for increase and $^{b}p<0.01$ vs. EC ^{wt} for decrease. Data were analyzed by ANOVA; Tukey HSD test for multiple comparisons.

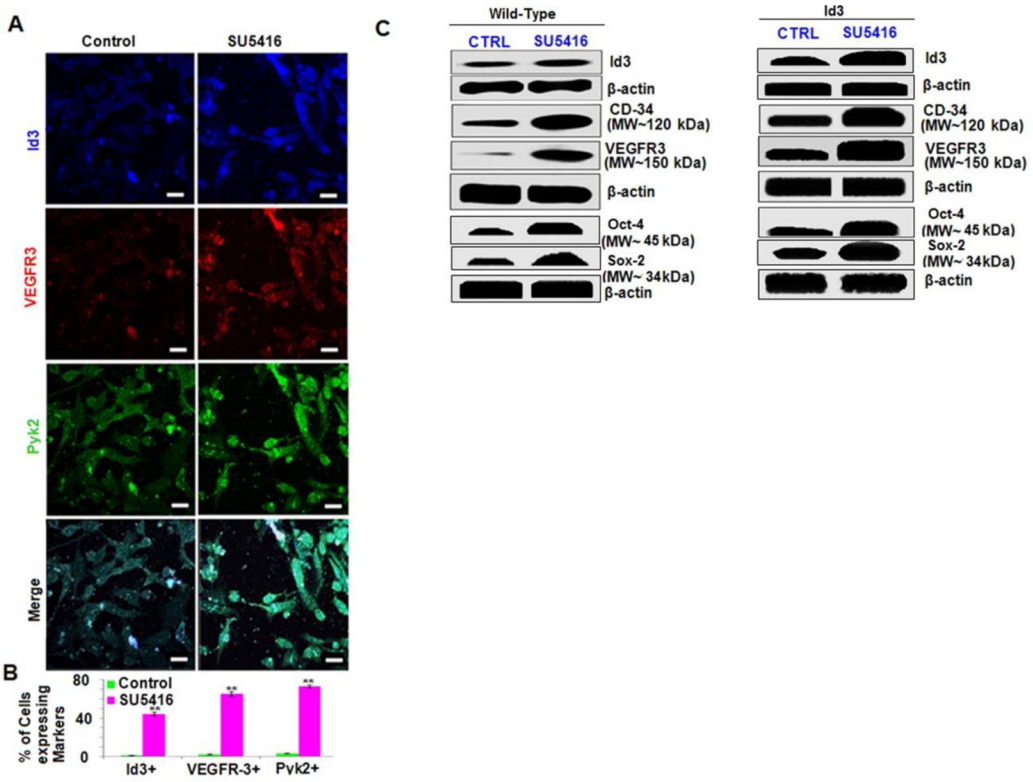

Fig. 3. SU5416-induced ID3, VEGFR3, and Pyk2 expression in microvascular ECs

EC ^{wt} was exposed to SU5416 [3μM] for 3h. Co-localization of target molecules was performed by immunofluorescence confocal microscopy. Cells were immunostained with antibodies against ID3 (blue), VEGFR3 (red), Pyk2 (green). (A) Immunofluorescent detection of ID3, VEGFR3, or Pyk2 in vehicle control (left panel) and SU5416 treated cells (right panel). Representative photomicrographs obtained by confocal microscopy are from one of three separate experiments. Scale bar = 70 μm (B) Percent of cells expressing each marker when treated with SU5416. EC ^{wt} exposed to SU5416 were 44% ID3^{+}, 65% VEGFR3^{+}, and 70% Pyk2^{+} compared to less than 5% in the vehicle control. The error bars represent the mean of expressed marker positive cells ± SD in 15 observed chambers of the slides. ** $p<0.01$ vs. control. Data were analyzed by ANOVA; Tukey HSD test for multiple comparisons. (C) Western blots for ID3, VEGFR3, Sox2, Oct4, and CD34 were used to determine SU5416-induced protein expression in treated EC ^{wt} and EC $^{ID3+}$.

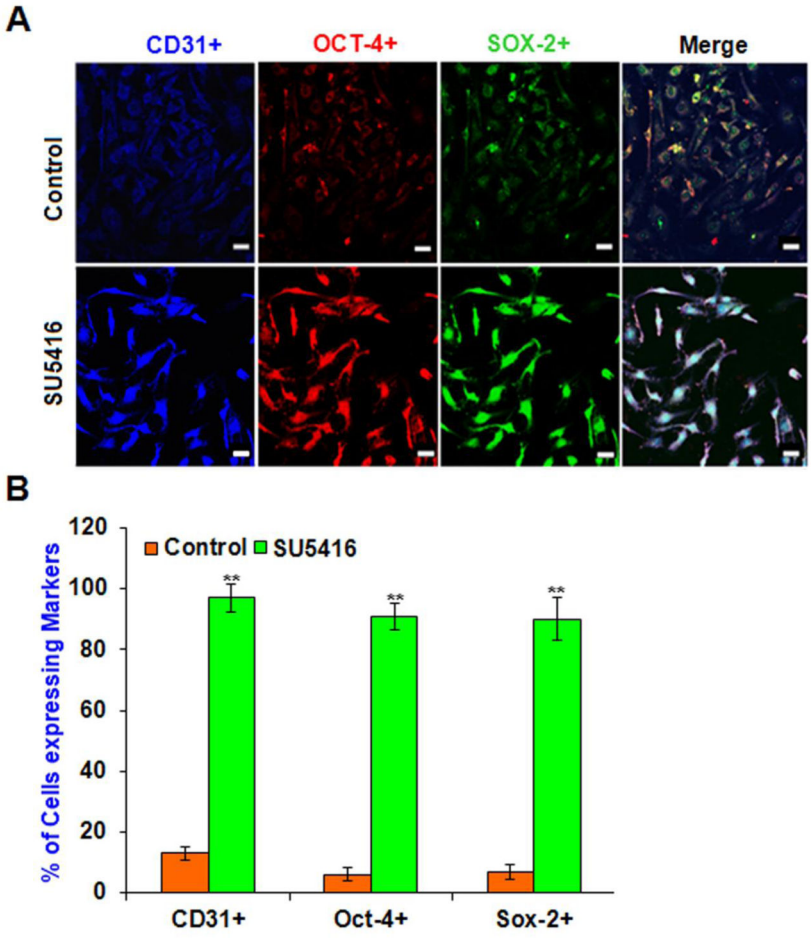

Fig. 4.

Pluripotent transcription factors Oct-4 and Sox-2 are induced by SU5416 in microvascular ECs. Since *in vivo* SU5416 exposure was recently reported to produce Oct-4^{+} cells within lung vascular lesions, we determined whether Oct-4 and Sox-2 expression increased in EC ^{wt} when exposed to SU5416. Cells were treated with SU5416 [5μM] for 3h and then cultured in fresh media for four days. Cells were immunostained with antibodies against CD31 (blue), Oct-4 (red), Sox-2 (green). Co-localization of relevant molecules was performed by confocal microscopy after immunofluorescence staining. (A) Immunofluorescent detection of Oct-4, Sox-2, or CD31 in vehicle control (top row) and SU5416 treated cells (bottom row). Representative images are from one of three experiments. Scale bar = 70 μm (B) Percent of cells expressing each marker when exposed to SU5416. For each group, 100 immunofluorescent cells were counted. In control, the cells that were scored 1 IF were counted and expressed as a percentage. In SU5416 group, cells that were scored 2 IF and 3 IF were counted and expressed as a percentage as described in Materials and Methods section. EC ^{wt} exposed to SU5416 were approximately 90% positive for Oct-4 and Sox-2 compared to less than 10% in the vehicle control. There was 90% co-localization of endothelial marker CD31 with these transcription factors. The error bars represent the mean of expressed marker positive cells ± SD.

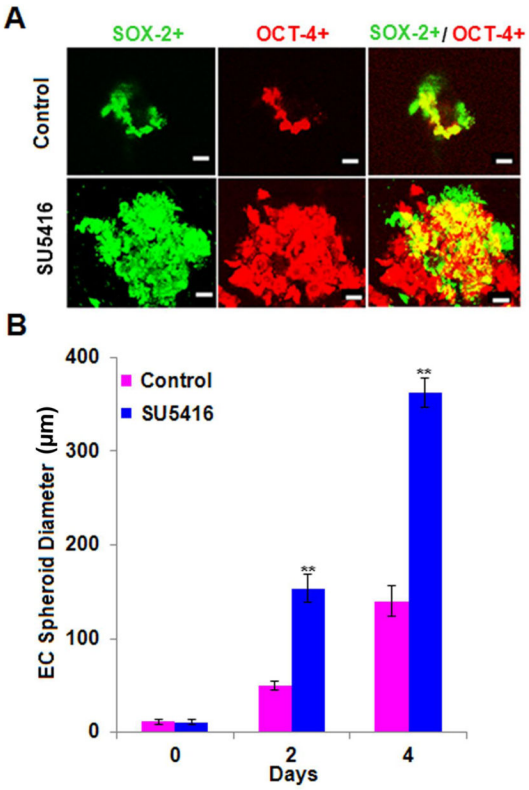

Fig. 5. SU5416 treated microvascular ECs form spheroids expressing Oct-4 and Sox-2

The novel conditions of treating EC ^{wt} with SU5416 in the sphere forming assay was used to verify chemical-induced pluripotent transcription factors observed previously in monolayer culture. EC ^{wt} were seeded at clonal density and cultured as spheroids in DMEM-F12 B27® serum-free media with or without SU5416 treatment. Cells were immunostained with antibodies against Oct-4 (red) and Sox-2 (green). Co-localization of relevant molecules was performed by confocal microscopy after immunofluorescence staining. (A) Immunofluorescent staining of Oct-4 and Sox-2 in EC ^{wt}. Vehicle control is shown in top row with SU5416 treated cells below. Representative images are from one of three experiments. Scale bar = 70 µm (B) Graph of EC ^{wt} spheroid diameter vs. time. SU5416 treatment showed a significant increase in spheroid diameter at days 2 and 4 when compared to vehicle control. The error bars represent the mean of expressed marker positive cells ± SD.

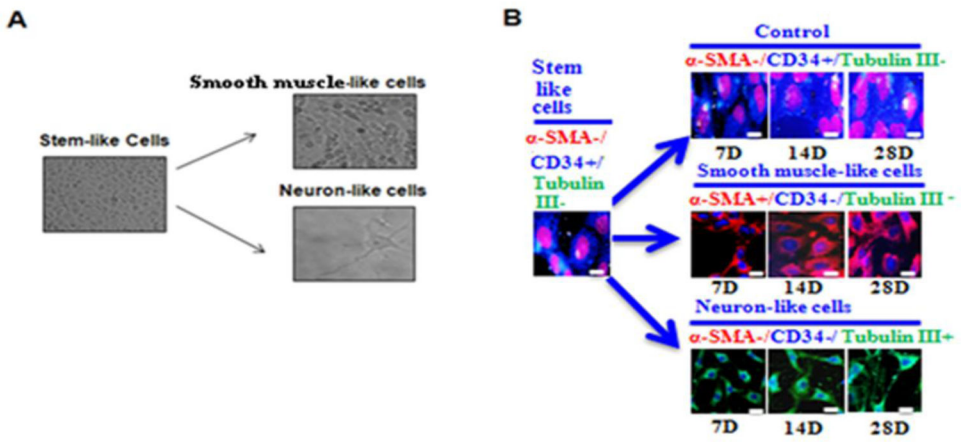

Fig. 6. EC $^{ID3+}$ stem-like cells display pluripotent morphology

(A) EC $^{ID3+}$ stem-like cells were differentiated under defined SMC or neuronal media. Images are from phase-contrast microscopy. EC $^{ID3+}$ were cultured as spheroids for 7d followed by 7d monolayer culture with differentiation medium. For SMC-like morphology spheroids were cultured with DMEM-F12 containing SMGS (Gibco). For neuron-like cells spheroids were cultured with Neurobasal® Medium (Gibco), StemPro® Neural Supplement (Gibco) and NGF-7s (Sigma). Magnification X 200. (B) Cell differentiation markers were determined using immunofluorescence at days 7, 14, and 28. For immunofluorescence imaging studies, slides were incubated with primary antibodies anti-CD34, α-smooth muscle actin (α-SMA), and β-tubulin III. Nuclei were counterstained with DRAQ5®. Scale bar=20μm. Images were captured with DeltaVision ELITE Olympus IX71 fluorescence microscope, Applied precision (Thermo Scientific) using software softWoRx-Acquire Version: 5.5.1 Release 3.

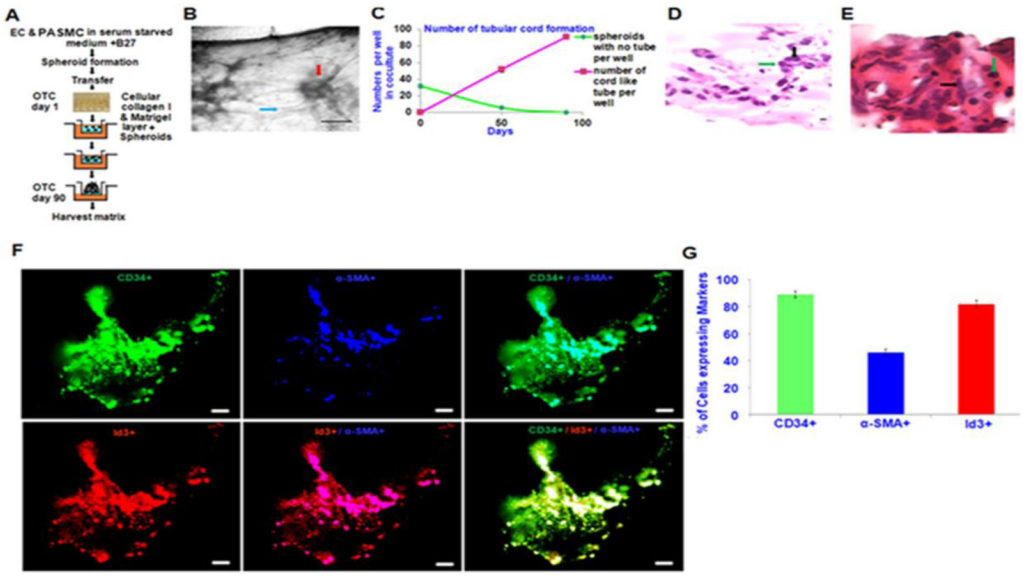

Fig. 7. EC $^{ID3+}$ form 3-D microvascular lesions

In vitro microvascular lesion formation by EC $^{ID3+}$ was determined in 3-D culture when grown with PASMCs. Both the EC ^{wt} and EC $^{ID3+}$ were seeded with PASMCs to form EC/SMC spheroids that were then transferred into well inserts containing a pre-cast 3-D gel matrix. Next, well inserts were cultured at 37°C for 90 days with a fresh change of serum-free DMEM-F12 supplemented with B27® every 15 days. (A) Diagrammatic representation of 3-D cell culture protocol. (B) Representative photomicrograph showing neovascularization and capillary-like formation among the spheroids in 3-D matrix. The spheroid indicated by the red arrow and capillary-like structure shown by the blue arrow. Scale bar=100 μm. (C) In graph, red line shows increasing number of tube structures from EC $^{ID3+}$/SMC spheroids per well during the 90 day time period. (D) Representative photomicrograph of the H&E stained tube-like structure. Green arrow indicates the small circular morphology of ECs while the black arrow indicates the bigger spindle shaped PASMCs. Scale bar=50 μm. (E) Representative photomicrograph of the H&E stained spheroid cross-section with intact cellular core and lumen-like structures. (F) Co-localization of EC with SMC was determined by confocal microscopy after immunofluorescent staining of cells with antibodies against endothelial marker CD34 (green), smooth muscle marker α-SMA (blue), and ID3 (red). Representative images (top panel) show SMCs organize along the capillary-like structures and ECs composed the spheroid core. Bottom panel shows co-localization of ID3 overexpression with EC marker CD34. (G) Graph depicts percent of cells expressing each marker. Approximately 45% of the cells immunostained positive for α-SMA, 90% stained positive for endothelial marker CD34, and 80% stained positive for ID3. The error bars represent the mean of expressed marker positive cells ± SD in slides.

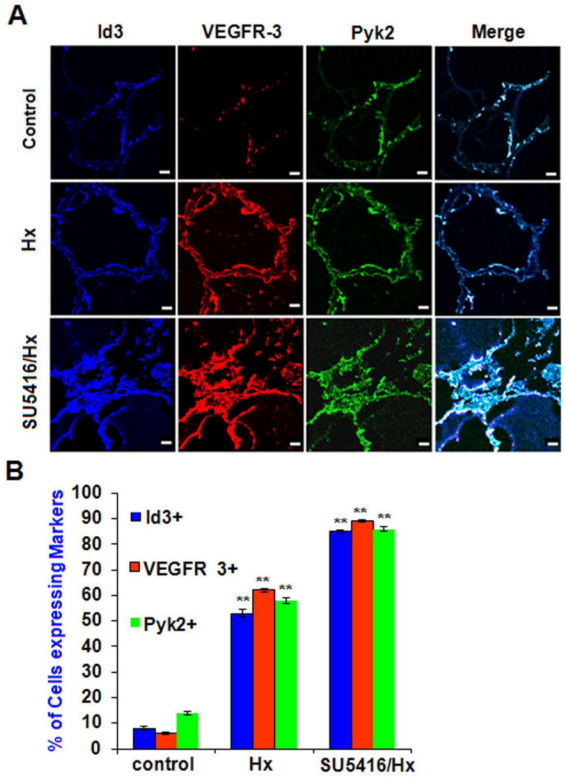

Fig. 8. In vivo pulmonary vascular lesions overexpress ID3, VEGFR3, and Pyk2

In vivo pulmonary vascular lesions overexpress ID3, VEGFR3, and Pyk2. Lung vascular lesions from the rodent SuHx model of severe PAH were stained with antibodies against: ID3 (blue), VEGFR3 (red), and Pyk2 (green) followed by immunofluorescent detection by confocal microscopy. (A) Both vehicle control and 3 wk chronic hypoxia treatment groups showed a uniform monolayer of cells lining the lumen of the pulmonary artery. SU5416-treated lungs exposed to chronic hypoxia for 3 wk (bottom row) showed a partially blocked lumen with cells stacked on top of each other instead of forming a monolayer. Representative images are from one of three lungs per group. Scale bar = 70 μm (B) Percent of cells expressing each marker amongst treatment groups when treated with vehicle control, hypoxia only, and SU5416 + hypoxia. Error bars represent the mean of expressed marker positive cells ± SD. ** $p<0.01$ vs. Control in normal/control (810), exposed in hypoxia and Sugen 5416/chronic hypoxia condition of lung tissue. Data were analyzed by ANOVA; Tukey HSD test for multiple comparisons.